

1 **Reduction of ferrihydrite with adsorbed and coprecipitated**
2 **organic matter: Microbial reduction by *Geobacter***
3 ***bremensis* versus abiotic reduction by Na-dithionite**

4
5 **K. Eusterhues¹, A. Hädrich², J. Neidhardt¹, K. Küsel^{2,3}, T. F. Keller^{4,*}, K. D.**
6 **Jandt⁴, K. U. Totsche¹**

7 [1]{Institut für Geowissenschaften, Friedrich-Schiller-Universität Jena, 07749 Jena,
8 Germany}

9 [2]{Institut für Ökologie, Friedrich-Schiller-Universität Jena, 07743 Jena, Germany}

10 [3]{German Centre for Integrative Biodiversity Research (iDiv) Halle-Jena-Leipzig, 04103
11 Leipzig, Germany}

12 [4]{Chair of Materials Science, Otto Schott Institute of Materials Research, Faculty of
13 Physics and Astronomy, Friedrich-Schiller-University Jena, 07743 Jena, Germany}

14 [*]{now at: Deutsches Elektronen-Synchrotron DESY, 22607 Hamburg, Germany}

15 Correspondence to: K. Eusterhues (karin.eusterhues@uni-jena.de)

16
17 **Abstract**

18 Ferrihydrite is a widespread poorly crystalline Fe oxide which becomes easily coated by
19 natural organic matter in the environment. This mineral-bound organic matter entirely
20 changes the mineral surface properties and therefore the reactivity of the original mineral.
21 Here, we investigated 2-line ferrihydrite, ferrihydrite with adsorbed organic matter, and
22 ferrihydrite co-precipitated with organic matter for microbial and abiotic reduction of Fe(III).
23 ferrihydrite-organic matter associations with different organic matter-loadings were reduced
24 either by *Geobacter bremensis* or abiotically by Na-dithionite. Both types of experiments
25 showed decreasing initial Fe reduction rates and decreasing degrees of reduction with
26 increasing amounts of mineral-bound organic matter. At similar organic matter-loadings,
27 coprecipitated ferrihydrites were more reactive than ferrihydrites with adsorbed organic
28 matter. The difference can be explained by the smaller crystal size and poor crystallinity of
29 such coprecipitates. At small organic matter loadings this led to even faster Fe reduction rates
30 than found for pure ferrihydrite. The amount of mineral-bound organic matter also affected
31 the formation of secondary minerals: goethite was only found after reduction of organic

32 matter-free ferrihydrite and siderite was only detected when ferrihydrites with relatively low
33 amounts of mineral-bound organic matter were reduced. We conclude that direct contact of *G.*
34 *bremensis* to the Fe oxide mineral surface was inhibited by attached organic matter.
35 Consequently, mineral-bound organic matter shall be taken into account as a factor in slowing
36 down reductive dissolution.

37

38 **1 Introduction**

39 Natural Fe oxides are typically nanoparticles and contribute significantly to the total surface
40 area and reactivity of a soil (Karlton et al., 2000; van der Zee et al., 2003; Eusterhues et al.,
41 2005; Regelink et al., 2013). Due to their high reactivity towards dissolved organic matter
42 (Torn et al., 1997; Kaiser and Zech 2000) Fe oxides are partially or completely covered by
43 organic matter in natural environments. Organic coverage may result in surfaces properties
44 strongly different from those of the original oxides, with consequences for aggregation,
45 mobility, and solubility.

46 One of the most common Fe oxides is poorly crystalline ferrihydrite, usually forming
47 aggregates of nanometer-sized individual crystals (Jambor and Dutrizac, 1998; Bigham et al.,
48 2002; Cornell and Schwertmann, 2003). In contrast to adsorption of organic matter on pre-
49 existing ferrihydrite surfaces, coprecipitation leads to adsorption and occlusion (physical
50 entrapment) of organic molecules in the interstices between the ferrihydrite crystals.
51 Additionally, the presence of dissolved organic matter inhibits ferrihydrite growth
52 (Schwertmann et al., 2005; Mikutta et al., 2008; Eusterhues et al., 2008; Cismasu et al., 2011),
53 and so coprecipitated ferrihydrites tend to develop smaller crystal sizes and more
54 crystallographic defects. Likewise, their aggregation behavior may be affected. Since
55 ferrihydrite is often formed in organic matter-rich solutions, e.g., in sediments and soils, we
56 assume that coprecipitation is a common process in nature. As coprecipitated ferrihydrites
57 differ in many properties from pure ferrihydrites, we suppose that the accessibility and
58 solubility of ferrihydrite surfaces as well as the accessibility of the adsorbed/occluded organic
59 matter to microorganisms, extracellular enzymes, redox active shuttling compounds or
60 reducing agents may differ from ferrihydrites with purely adsorbed organic matter.

61 In the past, dissolved humic acids from alkaline extracts have been added to microbial
62 experiments to test their influence on ferric iron reduction. It was suggested that they may
63 enhance Fe(III) reduction by electron shuttling (Lovley et al., 1996; Hansel et al., 2004; Jiang
64 and Kappler, 2008; Roden et al., 2010), complexation of Fe(II) (Royer et al., 2002) or

65 complexation and dissolution of Fe(III) (Jones et al., 2009). Amstaetter et al. (2012) and Jiang
66 and Kappler (2008) observed that the concentration of humic acid or the mineral/humic acid
67 ratio may control whether humic acids increase reduction or not. At high Fh concentrations in
68 solution (30mM), Amstaetter et al. (2012) even observed a decrease in Fe(III) reduction due
69 to humic acid addition. The decrease was explained by an increased aggregation and a
70 therefore reduced accessibility of the Fe oxide surface for bacteria. The influence of mineral-
71 bound organic matter on reduction and mineral transformation is less well investigated. We
72 are aware of only three articles: Henneberry et al. (2012) coprecipitated ferrihydrite with
73 dissolved organic matter from an agricultural drain and exposed the products to S(-II) and
74 Fe(II). Neither a release of the mineral-associated organic matter nor a mineral transformation
75 was observed during reduction. Pédrot et al. (2011) produced nanometer-sized lepidocrocite
76 and Fe-humic acid coprecipitates and compared its reduction by *Shewanella putrefaciens*.
77 They found the reduction of the coprecipitates to be about eight times faster than that of pure
78 lepidocrocite. Shimizu et al. (2013) studied the influence of coprecipitated humic acid on
79 ferrihydrite reduction by *Shewanella putrefaciens* strain CN32. Low C/Fe ratios were reported
80 to decrease the reduction of the ferrihydrite-humic acid associations, whereas an increased
81 reactivity was found at high C/Fe ratios. In addition, the mineral-bound humic acid changed
82 the mineral transformation during reduction. The formation of goethite was inhibited, the
83 formation of magnetite decreased and the formation of a green rust-like phase stimulated
84 (Shimizu et al., 2013). Such changes in the mineral assemblage will strongly affect the
85 cycling of Fe.

86 Our study aims to enlighten changes in microbial and abiotic Fe(III) reduction caused by
87 mineral-bound organic matter. A water extract of a Podzol forest floor was used as organic
88 matter and served to represent dissolved soil organic matter. We produced ferrihydrites with
89 different organic matter loadings by adsorption and coprecipitation, which were then exposed
90 to microbial reduction by *Geobacter bremensis* and chemical reduction by Na-dithionite.
91 *Geobacter bremensis* is common in soil and serves as a well investigated model organism for
92 dissimilatory Fe(III) reduction. Main objectives were to find out whether mineral-bound
93 organic matter increases or decreases ferrihydrite reactivity and whether coprecipitates differ
94 in reactivity from ferrihydrites with adsorbed organic matter. The formation of secondary
95 minerals was followed by XRD.

96

97 **2 Methods**

98 **2.1 Materials**

99 All chemicals used in this study are reagent grade. For preparation of stock solution and
100 media, 18 M Ω doubly deionized water was used. *Geobacter bremensis* (DSM 12179; Straub
101 & Buchholz-Cleven, 2001) was obtained from the German Resource Centre for Biological
102 Material (DSMZ, Braunschweig).

103

104 **2.2 Extraction of soil organic matter**

105 A forest floor extract was obtained from the Oa and Oe layers of a Podzol under spruce close
106 to Freising, Germany. Forest floor samples were air-dried and passed through a 2-mm sieve to
107 remove coarse plant remnants. Aliquots of 150 g soil and 700 ml deionized H₂O were shaken
108 end-over-end for 16 hours at room temperature and then centrifuged. The supernatant was
109 pressure-filtered through polyvinylidene fluoride (Durapore; 0.45 μ m pore width)
110 membranes, concentrated in low temperature rotary evaporators and freeze-dried. The C and
111 N concentration of the forest floor extract was measured using a CN analyzer (Vario EL,
112 Elementar Analysensysteme, Hanau, Germany). A transmission FTIR spectrum was collected
113 using the Nicolet iS10 (Thermo Fisher Scientific, Dreieich, Germany; see below). A solid-
114 state ¹³C NMR spectrum was acquired with a Bruker DSX-200 NMR spectrometer (Bruker
115 BioSpin, Karlsruhe, Germany), applying cross polarization with magic angle spinning (CP
116 MAS) at a spinning frequency of 6.8 kHz and a contact time of 1 ms. A ramped ¹H pulse was
117 used during contact time to circumvent spin modulation of Hartmann-Hahn conditions. Pulse
118 delays between 200 and 2000 ms were chosen.

119 **2.3 Synthesis of ferrihydrite and ferrihydrite-organic matter associations**

120 Two-line ferrihydrite was produced by titrating a 0.01 M Fe(NO₃)₃ solution with 0.1 M NaOH
121 to pH 5 under vigorous stirring. A series of ferrihydrites with different amounts of adsorbed
122 organic matter were produced by mixing forest floor extract solutions of different C
123 concentrations with suspensions of freshly precipitated 2-line ferrihydrite at pH 5. The molar
124 C/Fe of the initial solutions was AFhA 0.4, AFhB 1.3, and AFhD 4.2. Coprecipitated
125 ferrihydrites were obtained by dissolving Fe(NO₃)₃ in forest floor extract solutions of
126 different concentrations and adding 0.1 M NaOH under vigorous stirring until a pH of 5 was
127 reached. The molar C/Fe of these initial solutions was CFhA 0.4, CFhB 1.3, and CFhD 4.2.
128 The solid/solution (g/L) ratio varied between 0.3 and 1.6 for all syntheses. The solid products
129 were separated by centrifugation, washed twice with deionized H₂O and freeze-dried. The C
130 concentration of these samples was analyzed with the CN analyzer (Vario EL, Elementar
131 Analysensysteme, Hanau, Germany). Transmission FTIR spectra were taken (Nicolet iS10,

132 Thermo Fisher Scientific, Dreieich, Germany) on pellets of 2 mg sample diluted with 200 mg
133 KBr between 4000 and 400 cm^{-1} , accumulating 32 scans at a resolution of 4 cm^{-1} . The spectra
134 were baseline corrected by subtracting a straight line running between the two minima of each
135 spectrum and normalized by dividing each data point by the spectrum's maximum. ~~The spectra
136 were baseline corrected by subtracting a straight line running between the two minima of each
137 spectrum and normalized by dividing each data point by the spectrum's maximum.~~ The second
138 derivative was calculated using the Savitzky-Golay algorithm over 19-23 points. The specific
139 surface area of the pure ferrihydrite was measured by N_2 gas adsorption (Autosorb1,
140 Quantachrome, Odelzhausen, Germany) and calculated according to the BET- equation from
141 11 data points in the relative pressure range of 0.05 to 0.3. Prior to the measurements the
142 sample was outgassed for at least 16 hours at 343 K in vacuum to remove adsorbed water
143 from the sample surfaces. X-ray photoelectron spectra (XPS) were recorded using a Quantum
144 2000 (PHI Co., Chanhassen, MN, USA) instrument with a focused monochromatic $\text{AlK}\alpha$
145 source (1486.7 eV) for excitation. For the high resolution spectra, the pass energy was set to
146 58.70 eV. After subtracting a Shirley-type background, P2p and N1s spectra were evaluated
147 by fitting single pseudo-Voigt profiles (Lorentz portion = 0.2) to the measured data. Fe2p
148 spectra were fitted by a pre-peak, a surface peak, and four multiplet peaks of decreasing
149 intensity as proposed by McIntyre and Zetaruk (1977) and Grosvenor et al. (2004) for high
150 spin Fe(III) compounds. Distances between multiplets were constrained to 1 eV, the FWHM
151 was set to 1.4 eV and the Lorentz portion of the pseudo-Voigt curves was 0.2. The C1s peak
152 was fitted using four pseudo-Voigt profiles with a fixed FWHM of 1.9 and a Lorentz portion
153 of 0.2. The distances between the peaks were fixed to 1.6, 1.6, and 1.1 eV from lower to
154 higher binding energies to distinguish the C1s binding states C-C, C-H, C-O, C-N, C=O, N-
155 C=O and O-C=O.

156 **2.4 Microbial reduction experiments**

157 Differences in reducibility of ferrihydrite and ferrihydrite-organic matter associations and
158 secondary mineralization were studied in liquid cultures inoculated with *G. brevensis*. A
159 defined freshwater medium based on the *Geobacter* medium ATCC 1957, containing 1.5 g L^{-1}
160 NH_4Cl and 0.1 g L^{-1} KCl was used. After autoclaving and cooling under an N_2/CO_2 (80/20
161 v/v) atmosphere, 30 ml L^{-1} of 1 M NaHCO_3 (autoclaved, CO_2), 10 ml L^{-1} Wolfe's vitamin
162 solution (ATCC 1957), 10 ml L^{-1} modified Wolfe's minerals (ATCC 1957) and sodium-
163 acetate (7 mM) as carbon source were added. Unless stated otherwise, added solutions were
164 prepared under anoxic (N_2) conditions and filter sterilized (0.2 μm , PVDF). NaH_2PO_4 from

165 the original recipe was not added to avoid interaction of PO_4^{3-} with ferrihydrite. The final
166 medium had a pH of 6.8. The pH was chosen because recommended for optimum growth of
167 *Geobacter*, by both the DSMZ (Medium 579, pH 6.7 to 7.0) as well as the ATCC (Medium
168 1957, pH 6.8). Adsorption and coprecipitation experiments were performed at pH 5, i.e. under
169 pH conditions where most coprecipitates form in the presence of dissolved organic matter
170 (Eusterhues et al., 2011). However, the higher pH during reduction experiments may have
171 caused desorption of some of the mineral-bound organic matter.

172 The medium (10 ml) was dispensed under an N_2 gas stream into pre-sterilized (6 h 180 °C) 21
173 ml-culture tubes that contained pre-weighed ferrihydrite and ferrihydrite-organic matter
174 associations (40 mM per tube). After tubes were closed with butyl rubber stoppers and capped
175 with aluminium rings, they were flushed again with sterile N_2/CO_2 (80/20 v/v), applying an
176 overpressure of ~100 mbar. Pressure was monitored with a needle tensiometer (TensioCheck
177 TC1066, Tensiotechnik). Inoculation of ferrihydrite and ferrihydrite-organic matter
178 associations was performed with 4.8% (v/v; initial cell density $\sim 10^8 \text{ mL}^{-1}$) *G. bremensis* pre-
179 culture grown on phosphate-free medium with sodium-fumarate (50 mM) as electron acceptor
180 and sodium-acetate (20 mM) as electron donor and carbon source. Triplicate samples of all
181 treatments were incubated horizontally (30 °C) in the dark and shaken periodically.

182 For Fe(II) determination, 0.2 ml subsamples were taken anoxically from well shaken culture
183 tubes with a syringe and transferred into 0.5 M HCl for extraction (1 h in the dark). Fe(II) of
184 the extraction solutions was determined using the phenanthroline assay (Tamura et al., 1974).
185 Fe(total) was analyzed via ICP-OES (Spectroflame, Spectro, Kleve, Germany). Solid
186 remnants of the incubation experiments were freeze dried and stored under N_2 until XRD
187 measurements (D8 Advance DaVinci diffractometer by Bruker AXS, Karlsruhe, Germany)
188 were performed using $\text{Cu K}\alpha$ radiation at 40 kV and 40 mA.

189 **2.5 Abiotic reduction experiments with Na-dithionite**

190 Chemical reducibility of ferrihydrite and ferrihydrite-organic matter associations was
191 evaluated in abiotic reduction experiments performed after Houben (2003). In short,
192 ferrihydrite and ferrihydrite-organic matter associations (ca. 0.1 mmol Fe in ferrihydrite) were
193 added to 0.5 L of anoxic (N_2) 0.01 M Na-dithionite solution buffered with ca. 0.015 M
194 NaHCO_3 in a 1L screw cap bottle. Bottles were closed immediately with a rubber stopper and
195 a metal screw cap, shaken thoroughly and afterwards stirred constantly at room temperature.
196 The solution pH was adjusted to ~7 before ferrihydrite addition by shortly purging with CO_2
197 and was stable during the experiment. Periodically, samples of 0.5 ml were taken with N_2

198 flushed syringes and filtered through 0.2 µm membranes (PVDF) into cuvettes filled with 0.5
199 ml acetate (to quench the reduction) and ddH₂O (for dilution). The dissolved Fe(II) was
200 measured using the phenantroline method (Tamura et al., 1974).

201 **2.6 Evaluation of reduction rates:**

202 Fe(II) formation kinetics were used as analogues for Fe(III) reduction. Apparent initial
203 reaction rates were estimated by fitting linear regression lines to Fe(II)/Fe(total) versus time
204 for the first data points acquired in microbial and abiotic reduction experiments. The slope of
205 the line represents the initial reaction rate. The degree of dissolution was determined at day 17
206 for microbial experiments and after 75 min for abiotic experiments. Day 17 for microbial
207 experiments was chosen, because the Fe(II)/Fe(total) of the ferrihydrite control at day 52 is
208 much lower than at day 17 and therefore probably wrong. We assume that this is due to
209 unintentional oxidation at the end of the experiment in this sample. The data were fit also to a
210 model proposed first by Christoffersen and Christoffersen (1976) and used successfully by
211 e.g. Postma (1993), Larsen and Postma (2001), Houben (2003), and Roden (2004):

$$212 \quad m_t / m_0 = [-k(1-\gamma)t + 1]^{1/(1-\gamma)}$$

213 where m_0 is the initial concentration of Fe(III), m_t the concentration of Fe(II) at time t , k the
214 rate constant, and γ a constant describing the Fe mineral reactivity as controlled by crystal
215 size, morphology, structure and available reactive surface sites (Postma, 1993; Roden, 2004).
216 While we were successful in fitting the abiotic variants, the model failed to reconstruct the
217 biotic dissolution variants (data not shown). This may point to other processes involved in the
218 biotic dissolution, e.g., a preferential selection of a size fraction of the ferrihydrite-organic
219 matter-associations. However, the comparably poor data quality of the biotic variants does not
220 allow for an in-depth interpretation of this finding.

221

222 **3 Results and Discussion**

223 **3.1 Characterization of forest floor extract, control ferrihydrite and ferrihydrite- 224 organic matter associations**

225 The forest floor extract for the production of ferrihydrite-organic matter associations was
226 characterized by its C/N ratio, solid state ¹³C NMR (Figure 1) and FTIR (Figure 2). The
227 concentrations of C and N were found to be 35.1% and 4.3%. Organic C in the respective
228 chemical shift regions of the NMR spectrum was quantified to 13% of TOC alkyl C (0-45
229 ppm), 51% of TOC O-alkyl C (45-110 ppm), 24% of TOC aryl C (110-160 ppm), and 13% of

230 TOC carbonyl C (160-220 ppm). In comparison to the material used for previous adsorption
231 and coprecipitation studies (Eusterhues et al., 2008; Eusterhues et al., 2011; Eusterhues et al.,
232 2014) this material had a higher content in aromatic groups and carbonyl C (ester, carboxyl or
233 amide groups), and less carbohydrates. The FTIR spectrum (Figure 2; band assignment
234 according to Abdulla et al., 2010) shows strong peaks at 1722 cm^{-1} (C=O of COOH), 1622
235 cm^{-1} (complexed COO^-) and at 1148, 1089, and 1041 cm^{-1} (C-O in carbohydrates). Very sharp
236 signals at 1384 and 825 cm^{-1} are caused by NO_3^- , and show that only part of the N can belong
237 to amides. Additional smaller signals can be identified using the second derivative of the
238 spectrum: the signal at 1783 cm^{-1} points to the C=O stretching of γ -lactones, signals at 1547
239 and 1268 cm^{-1} can be explained by amide II and amide III, signals at 1512 and 1218 cm^{-1} are
240 in accordance with the C=C stretching of aromatic rings and with the asymmetric C-O
241 stretching of aromatic OH. The signal at 965 cm^{-1} belongs to the O-H out of plane bending of
242 carboxylic acids and the band at 660 cm^{-1} to the O-H out of plane bending of carbohydrates.

243 The control ferrihydrite as well as the ferrihydrites in coprecipitates and adsorption complexes
244 displayed XRD patterns of a typical 2-line ferrihydrite (Cornell and Schwertmann, 2003). The
245 specific surface area of the control ferrihydrite was 197 $\text{m}^2 \text{g}^{-1}$ as determined by N_2 gas
246 adsorption and the concentrations of C and N were found to be 0.2% and 1.3%. The FTIR
247 spectrum (Figure 2) showed that this high N concentration is due to nitrate, which has not
248 been fully removed during ferrihydrite synthesis from $\text{Fe}(\text{NO}_3)_3 \cdot 9 \text{H}_2\text{O}$. [Because *Geobacter*
249 *bremensis* is not able to reduce nitrate (Straub et al., 1998; Straub et al., 2001), we assume
250 that the nitrate contamination does not affect our microbial reduction experiments.]

251 The adsorption isotherm (Figure 3) can be described by a BET model (Ebadi et al., 2009) with
252 a monolayer adsorption capacity of $q_m=0.52 \text{ mg m}^{-2}$, an equilibrium constant of adsorption for
253 the first layer of $K_S = 0.9 \text{ L mg}^{-1}$, and an equilibrium constant of adsorption for further layers
254 of $K_L= 0.0045 \text{ L mg}^{-1}$. The obtained monolayer loading is in accordance with other adsorption
255 studies involving natural organic matter adsorption and ferrihydrite (Tipping et al., 1981;
256 Kaiser et al. 2007; Eusterhues et al., 2005). Coprecipitation, in contrast, produced
257 considerably larger organic matter-loadings of $\sim 1.1 \text{ mg m}^{-2}$. This can be explained either by a
258 larger surface area of coprecipitated ferrihydrites or by the presence of occluded organic
259 matter in addition to adsorbed organic matter in coprecipitates. Such a behavior was
260 previously reported for the coprecipitation of lignin, but not for a forest floor extract
261 (Eusterhues et al., 2011).

262 Three samples of each adsorption and the coprecipitation series were selected for the
263 reduction experiments (Table 1).

264 FTIR-spectra of adsorbed and coprecipitated organic matter differ from the original forest
265 floor extract. The peak assigned to C=O in protonated carboxyl groups (1723 cm^{-1}) is reduced
266 to merely a shoulder (seen only in the 2nd derivative of AFhD and CFhD at 1716 and 1712
267 cm^{-1}), while the signal related to deprotonated carboxyl groups (1622 cm^{-1} in FFE) is
268 increased and shifted to higher wavenumbers (1632 , 1631 cm^{-1}). This pattern is explained by
269 the formation of inner-sphere surface complexes between carboxylic acids and Fe oxides
270 surfaces or dissolved metals (Kang et al., 2008; Persson and Axe, 2005). The peak at 1148
271 cm^{-1} (C-O in carbohydrates) in the forest floor extract is not visible in the adsorbed or
272 coprecipitated organic matter and the peak at 1089 cm^{-1} is slightly shifted to lower
273 wavenumbers (1082 , 1079 cm^{-1}). Both changes point to a fractionation of carbohydrates
274 during adsorption or coprecipitation. The absence of the sharp peaks at 1384 and 825 cm^{-1}
275 shows that coprecipitates and adsorption complexes are free of nitrate. We assume, the
276 adsorption of organic matter has removed the surface bound nitrate, which could not be
277 removed from ferrihydrite through washing (Fh in Figure 2), and the natural nitrate from the
278 forest floor extract did not react with the Fe oxides (FFE in Figure 2).

279 FTIR spectra and their second derivatives of adsorbed and coprecipitated organic matter are
280 remarkably similar. Small differences however exists for the main carbohydrate peak and its
281 shoulders, but seem mainly related to the amount of mineral-bound organic matter: While
282 carbohydrates are represented by peaks at ~ 1125 and ~ 1080 and $\sim 1040\text{ cm}^{-1}$ in samples with
283 small C concentrations (AFhA; CFhA), samples with large C concentration show a strong
284 peak at $\sim 1080\text{ cm}^{-1}$ and a shoulder at $\sim 1040\text{ cm}^{-1}$ (AFhD, AFhB, CFhD).

285 The highly surface-sensitive XPS technique provides the chemical composition of typically
286 less than 10 nm of the sample surface (Seah and Dench, 1979).). High resolution XPS spectra
287 of the C1s, N1s, Fe2p, and P2p lines are given in Figure 4. Weak S2p signals (data not
288 shown) above the detection limit were found for the forest floor extract and for coprecipitates
289 and adsorption complexes with low C concentrations ($< 115\text{ mg/g}$). The absence of S in
290 complexes with higher organic matter contents may imply that adsorption of the forest floor
291 organic material outcompetes adsorption of sulfate. The N1s and the P2p peaks show
292 considerable noise (Figure 4), which leads to large scatter for C/N and C/P ratios (Figure 5).
293 Nevertheless, the data show that the C/N ratio and the C/P ratio of coprecipitates and
294 adsorption complexes are clearly higher than that of the original forest floor extract. While

295 C/P-ratios for the coprecipitated organic matter are very similar to that of the adsorbed
296 organic matter, a slightly, but significantly higher mean C/N-ratio (40) for the adsorbed
297 organic matter is observed in comparison to a C/N of 35 for coprecipitated organic matter (α
298 = 0.05; T-test). The C1s peak can be deconvoluted into four peaks as shown exemplary for the
299 forest floor extract (Figure 4) and assigned to 285.0 eV: C-C and C-H; 286.6 eV: C-O and C-
300 N; 288.2 eV: C=O and N-C=O, and 289.3 eV: O-C=O (Arnarson and Keil, 2001). The
301 adsorbed and coprecipitated organic matter was found enriched in aliphatic C (C-C, C-H) and
302 carboxylic C (O-C=O), but compositional differences between adsorbed and coprecipitated
303 cannot be seen (data not shown).

304 To find out whether the exposed ferrihydrite surface differs between coprecipitated
305 ferrihydrites and ferrihydrites with adsorbed organic matter, we determined the C/Fe-ratio
306 (Figure 5A). Although coprecipitated ferrihydrites might have occluded a major part of the
307 associated organic matter inside their aggregates, the XPS C/Fe-ratio was found to be similar
308 for samples with the same C concentration. We therefore assume that the accessibility of the
309 ferrihydrite surface for reducing agents or microbial cells is not systematically different in
310 coprecipitates and in ferrihydrites with adsorbed organic matter.

311

312 **3.2 Microbial Fe(III) reduction by *Geobacter bremensis***

313 Incubation of ferrihydrite-organic matter associations with *G. bremensis* (Figure 6) revealed
314 that reaction rates and degree of reduction varied with the amount of mineral associated
315 organic matter: Increasing organic matter-loadings on ferrihydrite led to decreasing initial
316 reaction rates and a decreasing degree of reduction for ferrihydrites with coprecipitated as
317 well as adsorbed organic matter (Table 1). Also, samples of the coprecipitation series were
318 more reactive than samples of the adsorption series, when comparing samples with
319 comparable organic matter contents. In case of AFhA, the sample with the smallest amount of
320 adsorbed organic matter (44 mg g⁻¹ C), the initial reaction rate was smaller (0.0017 min⁻¹)
321 than that of the organic matter-free control ferrihydrite Fh (0.0020 min⁻¹) while the degree of
322 dissolution at day 17 was similar (64%) to that of the control ferrihydrite (63%). In case of
323 CFhA, the ferrihydrite sample with the smallest amount of coprecipitated organic matter (44
324 mg g⁻¹ C), initial reaction rate (0.0021 min⁻¹) and degree of dissolution (82%) were even
325 larger than for the control ferrihydrite Fh.

326 We conclude that the mineral-bound organic matter results in a surface passivation of the
327 ferrihydrite surface. The fact that coprecipitates were more easily reduced than ferrihydrites

328 with adsorbed organic matter may be explained by smaller and more defective individual
329 ferrihydrite crystals in coprecipitates (Eusterhues et al., 2008) and a therefore larger specific
330 surface area. A possibly larger accessible outer ferrihydrite surface in coprecipitates compared
331 to ferrihydrite with the same amount of adsorbed organic matter can be ruled out based on
332 XPS results (Figure 5A). We assume that these effects dominate over the surface passivation
333 effect due to associated organic matter in case of the fast and extensive reduction of CFhA. A
334 systematically different aggregate structure between ferrihydrite with adsorbed organic matter
335 and coprecipitated ferrihydrites may also have influenced the availability of the mineral
336 surface (Pédrot et al., 2011). A possibly different composition of the mineral-bound organic
337 matter in coprecipitates compared to adsorption complexes is a further aspect, which has to be
338 taken into account. Although FTIR spectra and XPS spectra were very similar, we cannot
339 exclude differences between adsorbed and coprecipitated material. In a previous experiment
340 with a distinct forest floor extract (Eusterhues et al., 2011) FTIR spectra had also been very
341 similar, whereas ^{13}C NMR analyses of the non-reacted fraction had shown that the adsorbed
342 organic matter was enriched in O-alkyl C (carbohydrates), but depleted in carbonyl C and
343 alkyl C relative to the coprecipitated material. (It was not possible to obtain NMR spectra of
344 reasonable quality of the material used in this study. Formation of soluble Fe complexes in the
345 supernatant might be an explanation.) However, this knowledge does not help us to judge the
346 possibly different efficiency with which the possibly different fractions may inhibit
347 ferrihydrite reduction. The ability of molecules to form bi- or multinuclear inner-sphere bonds
348 was recognized to make strong inhibitors with respect to mineral dissolution (Stumm, 1997),
349 while the presence of electron accepting and electron donating groups in the organic material
350 controls its ability to act as an electron shuttle and promote reduction. Quinones and
351 condensed aromatic groups have been shown to be redox active in humic acids and chars
352 (Dunnivant et al., 1992; Scott et al., 1998; Klüpfel et al., 2014). While we do not expect any
353 condensed aromatics, we cannot quantify quinones or multinuclear inner-sphere bonds in the
354 mineral-bound organic matter.

355 Our microbial reduction results are surprisingly different from experiments performed by
356 Shimizu et al., (2013), who coprecipitated ferrihydrite with standard humic acids and
357 monitored reduction by *Shewanella putrefaciens* strain CN-32. They found that increasing
358 amounts of coprecipitated humic acid led to elevated microbial reduction. At high humic acid
359 loadings (C/Fe = 4.3) reduction rates based on dissolved Fe(II) were faster than that of pure
360 ferrihydrite, whereas lower humic acid loadings (C/Fe < 1.8) resulted in slower reduction
361 rates. Pure ferrihydrite was reduced at medium reduction rates. Although aggregate structure,

362 the ability of humic acid for ligand exchange and systematic changes in surface charge were
363 discussed to influence reduction kinetics, the experiments of Shimizu et al., (2013) are in
364 accordance with the overall assumption that the coprecipitated humic acid are used by
365 *Shewanella* to transfer electrons from the cell to Fe oxide and advance its electron shuttling
366 process. A threshold amount of ferrihydrite-associated humic acid was assumed to be
367 necessary before electron shuttling is larger than surface passivation by humic acid blocking
368 surface sites of ferrihydrite (Shimizu et al., 2013).

369 However, the enhancement of electron shuttling might have been especially strong for the
370 experimental conditions chosen by Shimizu et al. (2013), because the content of aromatic
371 groups and quinones is usually much larger in humic acid than in forest floor extracts as used
372 in this study. Accordingly, Piepenbrock et al. (2014) could show that the electron accepting
373 capacity, i.e. the concentration of redox-active functional groups, of a natural forest floor
374 extract was only half as high as that of the Pahokee Peat Humic Acid.

375 By comparing the two studies, the question arises if differences in electron transfer
376 mechanisms applied by the δ -Proteobacteria *Geobacter* and the γ -Proteobacteria *Shewanella*
377 can explain whether mineral-bound organic matter increases or decreases the reducibility of
378 Fe oxides. In general, the following electron transfer strategies have been discussed in the
379 literature: i) direct electron transfer (DET) by either membrane-bound redox-enzymes (Nevin
380 and Lovley, 2000) or bacterial nanowires (Reguera, et al., 2005; Gorby et al., 2006;
381 Malvankar et al., 2011) and ii) mediated electron transfer (MET) using either chelators (Nevin
382 and Lovley, 2002; Kraemer, 2004) or redox shuttling compounds that are produced by the cell
383 itself (Marsili et al., 2008) or are abundant in the extracellular environment (Lovley et al.,
384 1996). *Geobacter* has been found to require direct contact to the mineral surface, but is also
385 discussed to use nanowires for electron transfer (Malvankar et al., 2012; Boesen and Nielsen,
386 2013). *Geobacter* species can conserve energy from the transfer of electrons to a variety of
387 extracellular electron acceptors including metals like Mn(IV) and U(VI), but also electrodes
388 and humic acid. *Shewanella* is long known to not rely on direct contact (Arnold et al., 1990;
389 Caccavo et al., 1997; Lies et al., 2005) and to produce chelating compounds like flavins (von
390 Canstein, 2008). A study of Kotloski and Gralnick (2013) recently showed that flavin electron
391 shuttling but not direct electron transfer or nanowires is the primary mechanism of
392 extracellular electron transfer by *Shewanella oneidensis*.

393 For *Geobacter* increasing amounts of mineral-bound organic matter decreased reduction rates
394 and degree of reduction, probably because reactive surface sites of the mineral are blocked by

395 adsorbed organic matter molecules. Additionally, increasing amounts of organic matter will
396 increase the negative charge of the particle surface, which may also impede their accessibility
397 for negatively charged microbial cells (Shimizu et al., 2013 and ref. therein). For *Shewanella*
398 species, which use chelating agents and electron shuttles, smaller amounts of adsorbed
399 organic matter hinder reduction by passivation of reactive surface sites, whereas large
400 amounts of mineral-bound organic matter can be used to enhance electron shuttling or
401 chelating of Fe. Interestingly, we did not observe such an increase in reduction rates at very
402 large organic matter loadings, although also *Geobacter* species are able to reduce extracellular
403 organic matter. This can either be explained by the lower concentration of redox active groups
404 in natural dissolved organic matter compared to humic acid (Piepenbrock et al., 2014) or by
405 species dependent different capabilities.

406 Partial reduction of Fe oxides during microbial reduction is explained by surface passivation
407 by adsorption of Fe(II) (Roden and Urrutia, 1999, Liu et al., 2001). Our study similar to
408 Shimizu et al. (2013) shows that mineral-bound organic matter has to be taken into account as
409 an additional control of Fe(III) reduction. Because dissolved organic matter is present in
410 almost all natural environments such as lakes, wetlands and soils, the occurrence of mineral-
411 bound organic matter on Fe oxides is more likely than that of pure Fe oxides surfaces. Since
412 the precipitation of ferrihydrite usually takes place from organic matter-containing solutions,
413 the occurrence of coprecipitates is also more likely than that of ferrihydrite with only
414 adsorbed organic matter. For these coprecipitates, a smaller crystal size and a more defective
415 structure must be considered to result in faster reaction rates than compared to ferrihydrites
416 with similar amounts of adsorbed organic matter.

417 *Geobacteraceae* have been studied intensively and are thought to contribute significantly to
418 Fe(III)-reduction in most soils and sediments (Lovley, 2011 and ref. therein). Therefore we
419 believe the findings of this study might contribute to a better understanding of processes
420 occurring in a wide variety of environments.

421

422 **3.3 Mineral transformation during microbial reduction**

423 Investigating the solid remnants after 52 days of microbial reduction revealed that the
424 formation of secondary minerals has been affected by the presence of mineral-bound organic
425 matter (Table 2). Besides salts, such as halite, sal ammoniac and nahcolite, originating from
426 the medium, we detected the neo-formation of goethite (FeOOH) and siderite (FeCO₃).
427 Siderite was found after reduction of pure ferrihydrite (Fh) and in samples with rather low

428 amounts of organic matter (AFhA, CFhA, CFhB), goethite was only found after reduction of
429 the pure ferrihydrite. Thus, the formation of siderite was limited to experiments with high
430 reduction rates and high degrees of reduction, where the solubility product of siderite was
431 likely exceeded. The formation of goethite only took place in the absence of organic matter.
432 This is in accordance with the general observation that goethite formation is hindered by
433 organic matter (Schwertmann, 1966; Schwertmann, 1970) and with the experiments by
434 Henneberry et al. (2012), who reduced ferrihydrite-organic matter coprecipitates by S(-II) and
435 Fe(II) and observed no mineral transformation as well. Shimizu et al. (2013) also found
436 goethite only in the control experiments with pure ferrihydrite, whereas the reduction of
437 ferrihydrite-organic matter association favored the formation of green rust and magnetite.

438 Goethite formation during reduction is assumed to be catalyzed by Fe(II) ions which adsorb to
439 the Fe oxide surface (Hansel et al., 2003; Thompson et al., 2006; Yee et al., 2006). We
440 expected a competition of Fe(II) with organic matter and therefore a decreased amount of
441 goethite formation in our experiments. However, this does not explain that no goethite was
442 formed during the reduction of ferrihydrite in presence of only a small amount of mineral-
443 bound organic matter. Possible explanations could be the detection limit of XRD (~5%) and a
444 full coverage of Fe(II)-reactive sites on ferrihydrite (Shimizu et al., 2013). Furthermore, a
445 preferential reaction of Fe(II) with the mineral-bound organic matter instead of the Fe oxide
446 surface could be considered.

447

448 **3.4 Abiotic Reduction by Na-Dithionite**

449 During abiotic reduction with Na-dithionite (Figure 7, Table 1) we observed highest initial
450 reduction rates for the pure ferrihydrite and systematically decreasing reduction rates with
451 increasing amounts of mineral-bound organic matter. Likewise, the degree of reduction after
452 75 min is generally decreasing with increasing organic matter. An exception is sample CFhA,
453 for which the dissolved Fe(II) was estimated to be larger than the total Fe, which is not
454 possible. Therefore we did not calculate reduction rate and degree of reduction for this
455 sample. Reduction rates and the degree of reduction again tend to be larger for coprecipitated
456 ferrihydrite. Thus, abiotic reduction experiments displayed the same overall picture of the
457 reactivity of the ferrihydrite-organic matter associations as the microbial reduction
458 experiments with *G. bremensis*. However, reduction rates for Na-dithionite are two to three
459 orders of magnitude larger.

460 The data for abiotic reduction could be well represented by the model by Christoffersen and
461 Christoffersen (1976; Table 1). It is interesting to note that γ the parameter describing particle
462 shape, particle size, reactive site density and particle heterogeneity in this model is increasing
463 with increasing amounts of mineral-bound organic matter from 1.3 to 2.6 for coprecipitates
464 and from 2.9 to 7.4 for ferrihydrites with adsorbed organic matter (Table 1). Reduction of
465 pure ferrihydrite gave a γ of 2.4. The theoretical value for ideally dissolving isotropic particles
466 is $2/3$. Houben (2003) found a γ of 1.5 for reduction of ferrihydrite with Na-dithionite; Larsen
467 et al. (2006) reported values between 1 and 2.2 for reduction of aquifer material by ascorbic
468 acid. Roden (2004) observed a γ of 0.7 for synthetic ferrihydrite reduced by ascorbic acid and
469 values between 0.8 and 1.8 for natural Fe oxides. Reducing the same material microbially by
470 *Shewanella* led to much higher values of γ of 5.8 to 11.8. Likewise he observed lower degrees
471 of reduction for microbial reduction than for reduction by ascorbic acid. He concluded that the
472 low degrees of reduction as well as the high values for γ during microbial reduction reflect
473 “the inhibitory effect of Fe(II) accumulation on enzymatic electron transfer” (Roden, 2004).
474 However, because we observed high γ values for abiotic reduction (Table 1), we propose that
475 surface passivation by organic matter leads to a high γ , also.

476

477 **3.5 Summary and environmental implications**

478 Mineral-bound soil organic matter has been shown to decrease microbial reduction by *G.*
479 *bremensis* and abiotic reduction by Na-dithionite of ferrihydrite. The reactivity of
480 ferrihydrites with adsorbed organic matter differed from ferrihydrites coprecipitated with
481 organic matter: at similar organic matter contents higher initial reaction rates and higher
482 degrees of reduction were observed for coprecipitated ferrihydrites. Their higher reactivity
483 can be explained by the smaller crystal size and higher number of crystal defects due to
484 poisoning of crystal growth in the presence of organic matter during coprecipitation.
485 However, other aspects such as a different composition of the associated organic matter, a
486 different aggregate structure may also influence reduction kinetics. At low concentrations of
487 coprecipitated organic matter these effects may be stronger than the surface passivation by the
488 mineral-bound organic matter and lead to an even faster reduction of coprecipitates than of
489 pure ferrihydrite. We therefore propose that, in addition to the accumulation of Fe(II), the
490 organic matter coverage of Fe oxide surfaces is discussed as a further widespread mechanism
491 to slow down or cease enzymatic reduction.

492 The secondary formation of Fe minerals resulting from microbial reduction was also
493 influenced by the amount of mineral-bound organic matter. Goethite was only found after

494 reduction of the organic matter-free ferrihydrite and siderite was only detected when
495 ferrihydrites with relatively low amounts of mineral-bound organic matter were reduced. For
496 e.g. soils, where we assume that an organic matter covered Fe oxide surface is rather the rule
497 than the exception, we conclude that goethite and siderite formation is less likely than in
498 typical microbial reduction experiments. Growth of new minerals will influence the cycling of
499 Fe as well as of the usually associated nutrients and contaminants, because both goethite and
500 siderite represent thermodynamically more stable sinks for the fixation of Fe(III) and Fe(II)
501 than ferrihydrite and have different mineral surfaces.

502 Comparison to the studies of Pédrot et al. (2011) and Shimizu et al. (2013) let us assume that
503 the electron transfer mechanism of a microorganism controls whether or not mineral-bound
504 organic matter decreases or increases microbial reduction. Whereas *Shewanella* may use own
505 redox-active products to enhance electron shuttling, direct contact requiring *Geobacter* may
506 not be able to reach the oxide surface when blocked by organic matter. If this hypothesis
507 holds true, in natural environments, the likely presence of mineral-bound organic matter on Fe
508 oxide surfaces may increase or decrease Fe reduction, depending on the dominating types of
509 microorganisms. On the other hand, the composition or activity of the Fe reducing microbial
510 community might be regulated by the mean coverage of the Fe oxide surfaces. Systems with
511 low dissolved organic matter concentrations and low organic matter loadings on Fe oxides
512 might be favored by microorganisms requiring direct contact for reduction such as *Geobacter*,
513 whereas systems with high dissolved organic matter concentrations might be ideal for electron
514 shuttle or ligand driven microbial reduction.

515

516 **4 Conclusions**

517 Fe oxides are recognized as very important mineral phases, which protect their mineral-bound
518 organic matter against microbial degradation in the long-term. In redoximorphic soils, it will
519 depend on the type of reducing microorganism whether the presence of mineral-bound
520 organic matter will inhibit dissolution of the carrier mineral and support organic matter
521 storage at the same time. When direct electron transfer is the main mechanism for microbial
522 Fe(III) reduction, the organic matter coverage will protect the underlying Fe mineral and
523 promote its own preservation, whereas the opposite must be assumed for soils dominated by
524 microorganisms using electron shuttles or ligands for Fe(III) reduction.

525

526

527 **Acknowledgements**

528 Part of this work was financially supported by the priority program SPP 1315
529 “Biogeochemical Interfaces in Soil” of the Deutsche Forschungsgemeinschaft (DFG). Many
530 thanks to Angelika Kölbl, Markus Steffens and Ingrid Kögel-Knabner (Lehrstuhl für
531 Bodenkunde, Technische Universität München) for NMR-data and to Ralf Wagner (Chair of
532 Materials Science, University of Jena) for XPS measurements. We also highly appreciate help
533 in the laboratory by Katy Pfeiffer, Gundula Rudolph and Christine Götze.

534

535 **References**

- 536 Abdulla, H. A. N., Minor, E. C., Dias, R. F., and Hatcher, P. G.: Changes in the compound
537 classes of dissolved organic matter along an estuarine transect: A study using FTIR and C-
538 13 NMR, *Geochimica et Cosmochimica Acta*, 74, 3815-3838, 2010.
- 539 Amstaetter, K., Borch, T., and Kappler, A.: Influence of humic acid imposed changes of
540 ferrihydrite aggregation on microbial Fe(III) reduction, *Geochimica et Cosmochimica*
541 *Acta*, 85, 326-341, 2012.
- 542 Arnarson, T. S. and Keil, R. G.: Organic-mineral interactions in marine sediments studied
543 using density fractionation and X-ray photoelectron spectroscopy, *Organic Geochemistry*,
544 32, 1401-1415, 2001.
- 545 Arnold, R. G., Hoffmann, M. R., Dichristina, T. J., and Picardal, F. W.: Regulation of
546 Dissimilatory Fe(III) Reduction Activity in *Shewanella-Putrefaciens*, *Applied and*
547 *Environmental Microbiology*, 56, 2811-2817, 1990.
- 548 Bigham, J. M., Fitzpatrick, R. W., and Schulze, D. G.: Iron oxides. In: *Soil mineralogy with*
549 *environmental applications*, Dixon, J. B. and Schulze, D. G. (Eds.), SSSA Book Ser. No. 7,
550 Soil Science Society of America, Madison, WI, 2002.
- 551 Boesen, T. and Nielsen, L. P.: Molecular Dissection of Bacterial Nanowires, *Mbio*, 4, 2013.
- 552 Caccavo, F., Schamberger, P. C., Keiding, K., and Nielsen, P. H.: Role of hydrophobicity in
553 adhesion of the dissimilatory Fe(III)-reducing bacterium *Shewanella* alga to amorphous
554 Fe(III) oxide, *Applied and Environmental Microbiology*, 63, 3837-3843, 1997.
- 555 Christoffersen, J. and Christoffersen, M. R.: Kinetics of dissolution of calcium-sulfate-
556 dihydrate in water *Journal of Crystal Growth*, 35, 79-88, 1976.
- 557 Cismasu, A. C., Michel, F. M., Tcaciuc, A. P., Tyliczszak, T., and Brown, J., G.E.:
558 Composition and structural aspects of naturally occurring ferrihydrite, *Comptes Rendus*
559 *Geoscience*, 343, 210-218, 2011.
- 560 Cornell, R. M. and Schwertmann, U.: *The Iron Oxides: Structure, Properties, Reactions,*
561 *Occurrences and Uses*, Wiley-VCH Verlagsgesellschaft, Weinheim, 2003.
- 562 Dunnivant, F. M., Schwarzenbach, R. P., and Macalady, D. L.: Reduction of substituted
563 nitrobenzenes in aqueous-solution containing natural organic matter, *Environmental*
564 *Science & Technology*, 26, 2133-2141, 1992.
- 565 Ebadi, A., Mohammadzadeh, J. S. S., and Khudiev, A.: What is the correct form of BET
566 isotherm for modeling liquid phase adsorption? *Adsorption-Journal of the International*
567 *Adsorption Society*, 15, 65-73, 2009.

568 Eusterhues, K., Neidhardt, J., Hädrich, A., Küsel, K., and Totsche, K. U.: Biodegradation of
569 ferrihydrite-associated organic matter, *Biogeochemistry*, DOI 10.1007/s10533-013-9943-0,
570 2014.

571 Eusterhues, K., Rennert, T., Knicker, H., Kögel-Knabner, I., Totsche, K. U., and
572 Schwertmann, U.: Fractionation of Organic Matter Due to Reaction with Ferrihydrite:
573 Coprecipitation versus Adsorption, *Environmental Science & Technology*, 45, 527-533,
574 2011.

575 Eusterhues, K., Rumpel, C., and Kögel-Knabner, I.: Organo-mineral associations in sandy
576 acid forest soils: importance of specific surface area, iron oxides and micropores, *European*
577 *Journal of Soil Science*, 56, 753-763, 2005.

578 Eusterhues, K., Wagner, F. E., Häusler, W., Hanzlik, M., Knicker, H., Totsche, K. U., Kögel-
579 Knabner, I., and Schwertmann, U.: Characterization of Ferrihydrite-Soil Organic Matter
580 Coprecipitates by X-ray Diffraction and Mössbauer Spectroscopy, *Environmental Science*
581 *& Technology*, 42, 7891-7897, 2008.

582 Gorby, Y. A., Yanina, S., McLean, J. S., Rosso, K. M., Moyles, D., Dohnalkova, A.,
583 Beveridge, T. J., Chang, I. S., Kim, B. H., Kim, K. S., Culley, D. E., Reed, S. B., Romine,
584 M. F., Saffarini, D. A., Hill, E. A., Shi, L., Elias, D. A., Kennedy, D. W., Pinchuk, G.,
585 Watanabe, K., Ishii, S. i., Logan, B., Nealson, K. H., and Fredrickson, J. K.: Electrically
586 conductive bacterial nanowires produced by *Shewanella oneidensis* strain MR-1 and other
587 microorganisms, *Proceedings of the National Academy of Sciences of the United States of*
588 *America*, 103, 11358-11363, 2006.

589 Grosvenor, A. P., Kobe, B. A., Biesinger, M. C., and McIntyre, N. S.: Investigation of
590 multiplet splitting of Fe 2p XPS spectra and bonding in iron compounds, *Surface and*
591 *Interface Analysis*, 36, 1564-1574, 2004.

592 Hansel, C. M., Benner, S. G., Neiss, J., Dohnalkova, A., Kukkadapu, R. K., and Fendorf, S.:
593 Secondary mineralization pathways induced by dissimilatory iron reduction of ferrihydrite
594 under advective flow, *Geochimica et Cosmochimica Acta*, 67, 2977-2992, 2003.

595 Hansel, C. M., Benner, S. G., Nico, P., and Fendorf, S.: Structural constraints of ferric
596 (hydr)oxides on dissimilatory iron reduction and the fate of Fe(II), *Geochimica et*
597 *Cosmochimica Acta*, 68, 3217-3229, 2004.

598 Henneberry, Y. K., Kraus, T. E. C., Nico, P. S., and Horwath, W. R.: Structural stability of
599 coprecipitated natural organic matter and ferric iron under reducing conditions, *Organic*
600 *Geochemistry*, 48, 81-89, 2012.

601 Houben, G. J.: Iron oxide incrustations in wells. Part 2: chemical dissolution and modeling,
602 Applied Geochemistry, 18, 941-954, 2003.

603 Jambor, J. L. and Dutrizac, J. E.: Occurrence and constitution of natural and synthetic
604 ferrihydrite, a widespread iron oxyhydroxide, Chemical Reviews, 98, 2549-2585, 1998.

605 Jiang, J. and Kappler, A.: Kinetics of microbial and chemical reduction of humic substances:
606 Implications for electron shuttling, Environmental Science & Technology, 42, 3563-3569,
607 2008.

608 Jones, A. M., Collins, R. N., Rose, J., and Waite, T. D.: The effect of silica and natural
609 organic matter on the Fe(II)-catalysed transformation and reactivity of Fe(III) minerals,
610 Geochimica et Cosmochimica Acta, 73, 4409-4422, 2009.

611 Kang, S. H., Amarasiriwardena, D., and Xing, B. S.: Effect of dehydration on dicarboxylic
612 acid coordination at goethite/water interface, Colloid Surf. A-Physicochem. Eng. Asp.,
613 318, 275-284, 2008.

614 Kaiser, K., Mikutta, R., and Guggenberger, G.: Increased stability of organic matter sorbed to
615 ferrihydrite and goethite on aging, Soil Science Society of America Journal, 71, 711-719,
616 2007.

617 Kaiser, K. and Zech, W.: Dissolved organic matter sorption by mineral constituents of subsoil
618 clay fractions, Journal of Plant Nutrition and Soil Science, 163, 531-535, 2000.

619 Karlton, E., Bain, D. C., Gustafsson, J. P., Mannerkoski, H., Murad, E., Wagner, U., Fraser,
620 A. R., McHardy, W. J., and Starr, M.: Surface reactivity of poorly-ordered minerals in
621 podzol B horizons, Geoderma, 94, 265-288, 2000.

622 Klüpfel, L., Keiluweit, M., Kleber, M., and Sander, M.: Redox Properties of Plant Biomass-
623 Derived Black Carbon (Biochar), Environmental Science & Technology, 48, 5601-5611,
624 2014.

625 Kotloski, N. J. and Gralnick, J. A.: Flavin Electron Shuttles Dominate Extracellular Electron
626 Transfer by *Shewanella oneidensis*, Mbio, 4, 2013.

627 Kraemer, S. M.: Iron oxide dissolution and solubility in the presence of siderophores, Aquatic
628 Sciences, 66, 3-18, 2004.

629 Larsen, O. and Postma, D.: Kinetics of reductive bulk dissolution of lepidocrocite,
630 ferrihydrite, and goethite, Geochimica et Cosmochimica Acta, 65, 1367-1379, 2001.

631 Larsen, O., Postma, D., and Jakobsen, R.: The reactivity of iron oxides towards reductive
632 dissolution with ascorbic acid in a shallow sandy aquifer - (Romo, Denmark), Geochimica
633 et Cosmochimica Acta, 70, 4827-4835, 2006.

634 Lies, D. P., Hernandez, M. E., Kappler, A., Mielke, R. E., Gralnick, J. A., and Newman, D.
635 K.: *Shewanella oneidensis* MR-1 uses overlapping pathways for iron reduction at a
636 distance and by direct contact under conditions relevant for biofilms, *Applied and*
637 *Environmental Microbiology*, 71, 4414-4426, 2005.

638 Liu, C. X., Kota, S., Zachara, J. M., Fredrickson, J. K., and Brinkman, C. K.: Kinetic analysis
639 of the bacterial reduction of goethite, *Environmental Science & Technology*, 35, 2482-
640 2490, 2001.

641 Lovley, D. R., Coates, J. D., BluntHarris, E. L., Phillips, E. J. P., and Woodward, J. C.:
642 Humic substances as electron acceptors for microbial respiration, *Nature*, 382, 445-448,
643 1996.

644 Lovley, D. R., Ueki, T., Zhang, T., Malvankar, N. S., Shrestha, P. M., Flanagan, K. A.,
645 Aklujkar, M., Butler, J. E., Giloteaux, L., Rotaru, A.-E., Holmes, D. E., Franks, A. E.,
646 Orellana, R., Risso, C., and Nevin, K. P.: *Geobacter: The Microbe Electric's Physiology,*
647 *Ecology, and Practical Applications*. In: *Advances in Microbial Physiology*, Vol 59, Poole,
648 R. K. (Ed.), *Advances in Microbial Physiology*, 2011.

649 Malvankar, N. S., Tuominen, M. T., and Lovley, D. R.: Comment on "On electrical
650 conductivity of microbial nanowires and biofilms" by S. M. Strycharz-Glaven, R. M.
651 Snider, A. Guiseppi-Elie and L. M. Tender, *Energy Environ. Sci.*, 2011, 4, 4366, *Energy &*
652 *Environmental Science*, 5, 6247-6249, 2012.

653 Malvankar, N. S., Vargas, M., Nevin, K. P., Franks, A. E., Leang, C., Kim, B.-C., Inoue, K.,
654 Mester, T., Covalla, S. F., Johnson, J. P., Rotello, V. M., Tuominen, M. T., and Lovley, D.
655 R.: Tunable metallic-like conductivity in microbial nanowire networks, *Nature*
656 *Nanotechnology*, 6, 573-579, 2011.

657 Marsili, E., Baron, D. B., Shikhare, I. D., Coursolle, D., Gralnick, J. A., and Bond, D. R.:
658 *Shewanella* secretes flavins that mediate extracellular electron transfer, *Proceedings of the*
659 *National Academy of Sciences of the United States of America*, 105, 3968-3973, 2008.

660 McIntyre, N. S. and Zetaruk, D. G.: X-Ray Photoelectron Spectroscopic studies of iron
661 oxides, *Analytical Chemistry*, 49, 1521-1529, 1977.

662 Mikutta, C., Mikutta, R., Bonneville, S., Wagner, F., Voegelin, A., Christl, I., and
663 Kretzschmar, R.: Synthetic coprecipitates of exopolysaccharides and ferrihydrite. Part I:
664 Characterization, *Geochimica et Cosmochimica Acta*, 72, 1111-1127, 2008.

665 Nevin, K. P. and Lovley, D. R.: Lack of production of electron-shuttling compounds or
666 solubilization of Fe(III) during reduction of insoluble Fe(III) oxide by *Geobacter*
667 *metallireducens*, *Applied and Environmental Microbiology*, 66, 2248-2251, 2000.

668 Nevin, K. P. and Lovley, D. R.: Mechanisms for accessing insoluble Fe(III) oxide during
669 dissimilatory Fe(III) reduction by *Geothrix fermentans*, *Applied and Environmental*
670 *Microbiology*, 68, 2294-2299, 2002.

671 Pédrot, M., Le Boudec, A., Davranche, M., Dia, A., and Henin, O.: How does organic matter
672 constrain the nature, size and availability of Fe nanoparticles for biological reduction?
673 *Journal of Colloid and Interface Science*, 359, 75-85, 2011.

674 Persson, P. and Axe, K.: Adsorption of oxalate and malonate at the water-goethite interface:
675 molecular surface speciation from IR spectroscopy, *Geochimica et Cosmochimica Acta*,
676 69, 541-552, 2005.

677 Piepenbrock, A., Schröder, C., and Kappler, A.: Electron Transfer from Humic Substances to
678 Biogenic and Abiogenic Fe(III) Oxyhydroxide Minerals, *Environmental Science &*
679 *Technology*, 48, 1656-1664, 2014.

680 Postma, D.: The reactivity of iron-oxides in sediments - A kinetic approach, *Geochimica et*
681 *Cosmochimica Acta*, 57, 5027-5034, 1993.

682 Regelink, I. C., Weng, L., Koopmans, G. F., and Van Riemsdijk, W. H.: Asymmetric flow
683 field-flow fractionation as a new approach to analyse iron-(hydr)oxide nanoparticles in soil
684 extracts, *Geoderma*, 202, 134-141, 2013.

685 Reguera, G., McCarthy, K. D., Mehta, T., Nicoll, J. S., Tuominen, M. T., and Lovley, D. R.:
686 Extracellular electron transfer via microbial nanowires, *Nature*, 435, 1098-1101, 2005.

687 Roden, E. E.: Analysis of long-term bacterial vs. chemical Fe(III) oxide reduction kinetics,
688 *Geochimica et Cosmochimica Acta*, 68, 3205-3216, 2004.

689 Roden, E. E. and Urrutia, M. M.: Ferrous iron removal promotes microbial reduction of
690 crystalline iron(III) oxides, *Environmental Science & Technology*, 33, 2492-2492, 1999.

691 Roden, E. E., Kappler, A., Bauer, I., Jiang, J., Paul, A., Stoesser, R., Konishi, H., and Xu, H.
692 F.: Extracellular electron transfer through microbial reduction of solid-phase humic
693 substances, *Nature Geoscience*, 3, 417-421, 2010.

694 Royer, R. A., Burgos, W. D., Fisher, A. S., Jeon, B. H., Unz, R. F., and Dempsey, B. A.:
695 Enhancement of hematite bioreduction by natural organic matter, *Environmental Science*
696 *& Technology*, 36, 2897-2904, 2002.

697 Schwertmann, U.: Influence of various simple organic anions on formation of goethite and
698 hematite from amorphous ferric hydroxide, *Geoderma*, 3, 207-&, 1970.

699 Schwertmann, U.: Inhibitory effect of soil organic matter on crystallization of amorphous
700 ferric hydroxide, *Nature*, 212, 645-&, 1966.

701 Schwertmann, U., Wagner, F., and Knicker, H.: Ferrihydrite-humic associations: Magnetic
702 hyperfine interactions, *Soil Science Society of America Journal*, 69, 1009-1015, 2005.

703 Scott, D. T., McKnight, D. M., Blunt-Harris, E. L., Kolesar, S. E., and Lovley, D. R.:
704 Quinone moieties act as electron acceptors in the reduction of humic substances by
705 humics-reducing microorganisms, *Environmental Science & Technology*, 32, 2984-2989,
706 1998.

707 Seah, M. P. and Dench, W. A.: Quantitative electron spectroscopy of surfaces: A standard
708 data base for electron inelastic mean free paths in solids, *Surface and Interface Analysis*, 1,
709 2-11, 1979.

710 Shimizu, M., Zhou, J., Schroeder, C., Obst, M., Kappler, A., and Borch, T.: Dissimilatory
711 reduction and transformation of ferrihydrite-humic acid coprecipitates, *Environmental
712 Science & Technology*, 47, 13375-13384, 2013.

713 Straub, K. L., Hanzlik, M., and Buchholz-Cleven, B. E. E.: The use of biologically produced
714 ferrihydrite for the isolation of novel iron-reducing bacteria, *Systematic and Applied
715 Microbiology*, 21, 442-449, 1998.

716 Straub, K. L. and Buchholz-Cleven, B. E. E.: *Geobacter bremensis* sp nov and *Geobacter
717 pelophilus* sp nov., two dissimilatory ferric-iron-reducing bacteria, *International Journal of
718 Systematic and Evolutionary Microbiology*, 51, 1805-1808, 2001.

719 Stumm, W.: Reactivity at the mineral-water interface: Dissolution and inhibition, *Colloids
720 and Surfaces A- Physicochemical and Engineering Aspects*, 120, 143-166, 1997.

721 Tamura, H., Goto, K., Yotsuyan, T, and Nagayama, M.: Spectrophotometric determination of
722 iron(II) with 1,10-phenanthroline in presence of large amounts of iron(III), *Talanta*, 21,
723 314-318, 1974.

724 Thompson, A., Chadwick, O. A., Rancourt, D. G., and Chorover, J.: Iron-oxide crystallinity
725 increases during soil redox oscillations, *Geochimica et Cosmochimica Acta*, 70, 1710-
726 1727, 2006.

727 Tipping, E.: The Adsorption of Aquatic Humic Substances by Iron-Oxides, *Geochimica et
728 Cosmochimica Acta*, 45, 191-199, 1981.

729 Torn, M. S., Trumbore, S. E., Chadwick, O. A., Vitousek, P. M., and Hendricks, D. M.:
730 Mineral control of soil organic carbon storage and turnover, *Nature*, 389, 170-173, 1997.

731 von Canstein, H., Ogawa, J., Shimizu, S., and Lloyd, J. R.: Secretion of flavins by *Shewanella*
732 species and their role in extracellular electron transfer, *Applied and Environmental
733 Microbiology*, 74, 615-623, 2008.

734 van der Zee, C., Roberts, D. R., Rancourt, D. G., and Slomp, C. P.: Nanogoethite is the
735 dominant reactive oxyhydroxide phase in lake and marine sediments, *Geology*, 31, 993-
736 996, 2003.

737 Yee, N., Shaw, S., Benning, L. G., and Nguyen, T. H.: The rate of ferrihydrite transformation
738 to goethite via the Fe(II) pathway, *American Mineralogist*, 91, 92-96, 2006.

739

740

741

742

743 Table 1. Carbon concentration and C/Fe of ferrihydrite-organic matter associations and results

744 of microbial and abiotic reduction experiments.

		Reduction by <i>Geobacter brempensis</i>					Reduction by Na-dithionite					
		C	C/Fe	linear fit		degree of dissolution*	linear fit		degree of dissolution**	C&C		
				k	r ²		k	r ²		k	γ	r ²
mg/g	mol/mol	h ⁻¹		%	h ⁻¹		h ⁻¹					
control	Fh	2	0.02	0.0020	0.961	63	5.29	0.998	83	5.79	2.4	0.989
adsorbed OM	AFhA	44	0.39	0.0017	0.955	64	1.59	0.895	62	2.26	2.9	0.990
	AFhB	105	1.04	0.0011	0.965	42	0.72	0.895	30	1.07	7.2	0.991
	AFhD	181	2.46	0.0010	0.939	36	0.67	0.811	24	0.60	7.4	0.979
coprecipitated OM	CFhA	44	0.41	0.0021	0.950	82	-***	-	-	-	-	-
	CFhB	98	1.06	0.0016	0.983	68	1.09	0.975	64	1.32	1.9	0.995
	CFhD	182	2.83	0.0014	0.948	41	0.18	0.975	20	0.21	2.6	0.996

* degree of dissolution at day 17

**degree of dissolution at 75 min.

*** Please note that for the reduction by Na-dithionite for sample CFhA the dissolved Fe(II) was estimated to be larger than the total Fe, which is not possible. Therefore we did not calculate reduction rate and degree of reduction for this sample

745

746

747

748 Table 2. Mineral identification by XRD after reduction by *G. bremensis*. Sal ammoniac
 749 (NH₄Cl) is abbreviated by “sal”, nahcolite (NaHCO₃) by “nahc”.

		halite	sal	nahc	calcite	siderite	goethite
control	Fh	x	x	x	x	x	x
	AFhA	x				x	
adsorbed OM	AFhB	x	(x)*				
	AFhD	x	x				
	CFhA	x	x			x	
coprecipitated OM	CFhB	x	x	x		x	
	CFhD	x	x				

750 *(x) less than 3 peaks identified

751

752 **Figure captions**

753 Figure 1. ^{13}C CPMAS NMR spectrum of the forest floor extract.

754

755 Figure 2. FTIR spectra of the control ferrihydrite (Fh), the original forest floor extract (FFE),
756 the adsorption complexes (AFhD, AFhB, AFhA), and the coprecipitates (CFhD, CFhB,
757 CFhA). Second derivatives are given for spectra of the forest floor extract and the two
758 ferrihydrite-organic matter complexes with the highest C concentration.

759

760 Figure 3. Ferrihydrite-associated C (normalized to the specific surface area of $197\text{ m}^2\text{ g}^{-1}$ of
761 the control ferrihydrite) vs. C in the equilibrium solution. The line represents a BET-isotherm.

762

763 Figure 4. Background corrected XPS spectra of the control ferrihydrite (Fe2p, red), the forest
764 floor extract (C1s, N1s, P2p, blue) and the incubated coprecipitates and adsorption
765 complexes.

766

767 Figure 5. Comparison of chemical surface composition expressed in XPS signal ratios (C/Fe,
768 C/N, and C/P) and bulk C content of Fh-OM associations.

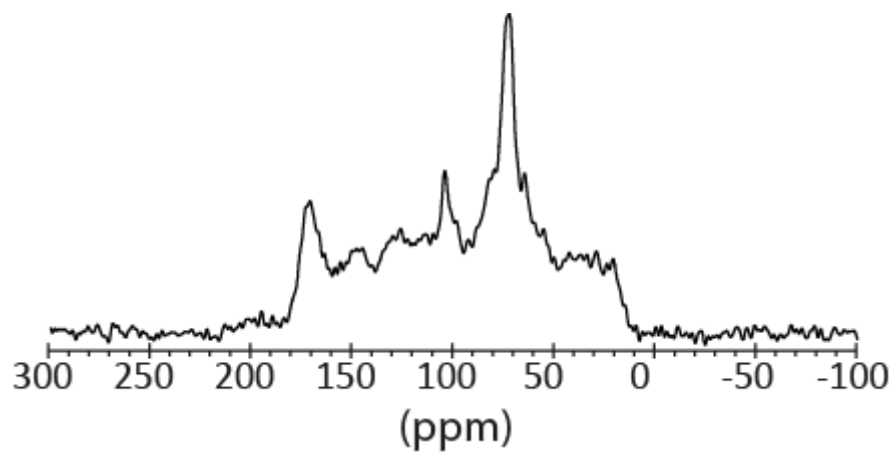
769

770 Figure 6. Microbial reduction of ferrihydrite and ferrihydrite-organic matter associations in
771 *Geobacter bremensis* cultures. The Fe(II) production was normalized to the total initial
772 amount of Fe in ferrihydrite. The Fe(II)/Fe(total) of the ferrihydrite control (red stars) at day
773 52 is much lower than at day 17 and therefore unexpectedly low, letting us assume that this is
774 due to unintentional oxidation at the end of the experiment in this sample. Error bars represent
775 standard deviations of triplicate cultures.

776

777 Figure 7. Abiotic reduction with Na-dithionite: Fe(II) production (normalized to the total
778 initial Fe in ferrihydrite) versus time. Lines represent the model by Christoffersen and
779 Christoffersen (1976). Note that the dissolved Fe(II) was estimated to be larger than the total
780 Fe for sample CFhA, which is unreasonable.

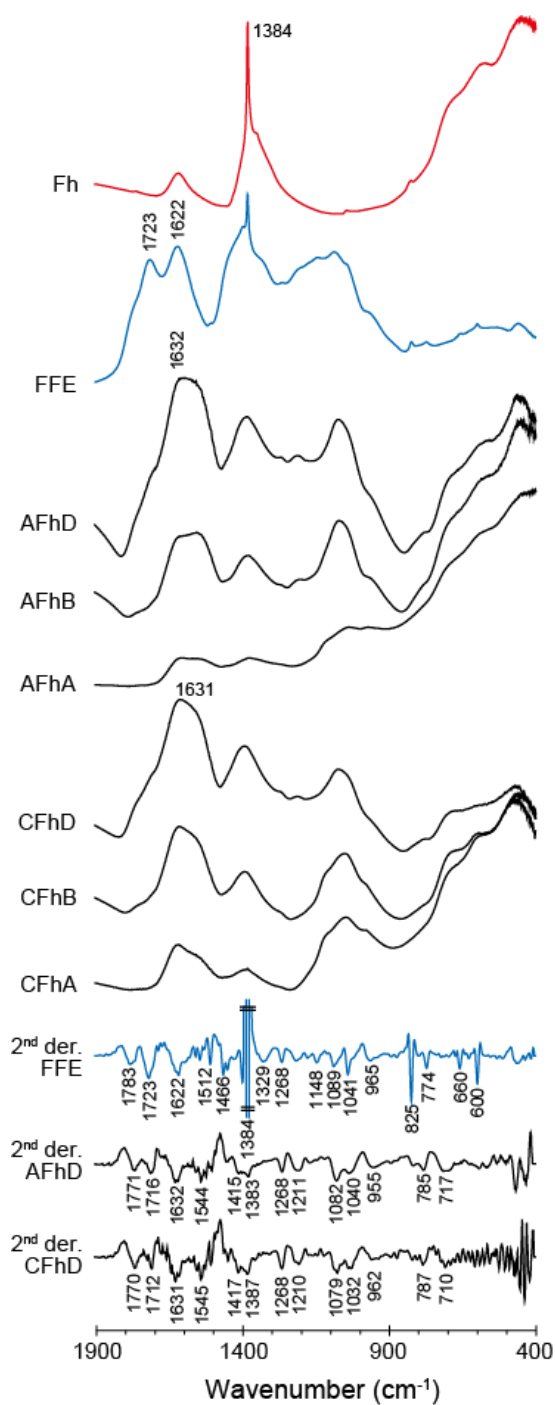
781



782

783

784 Figure 1. ¹³C CPMAS NMR spectrum of the forest floor extract.



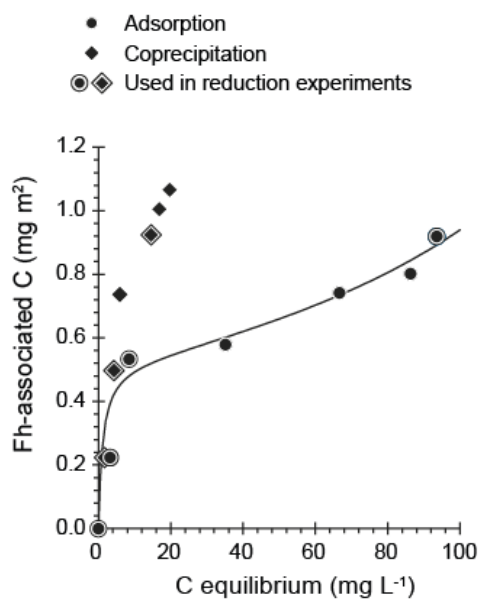
786

787 Figure 2. FTIR spectra of the control ferrihydrite (Fh), the original forest floor extract (FFE),
 788 the adsorption complexes (AFhD, AFhB, AFhA), and the coprecipitates (CFhD, CFhB,
 789 CFhA). Second derivatives are given for spectra of the forest floor extract and the two
 790 ferrihydrite-organic matter complexes with the highest C concentration.

791

792

793

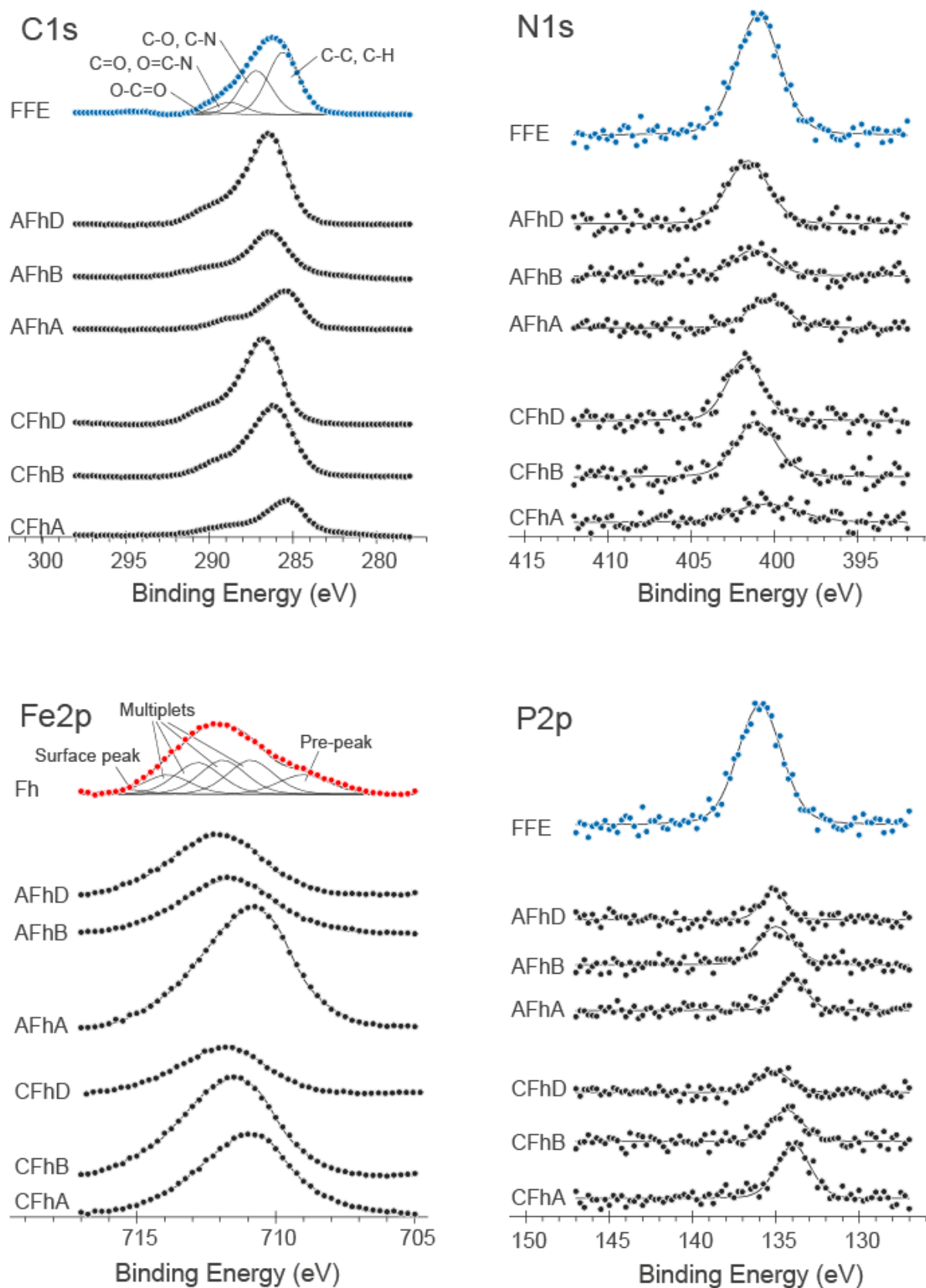


794

795

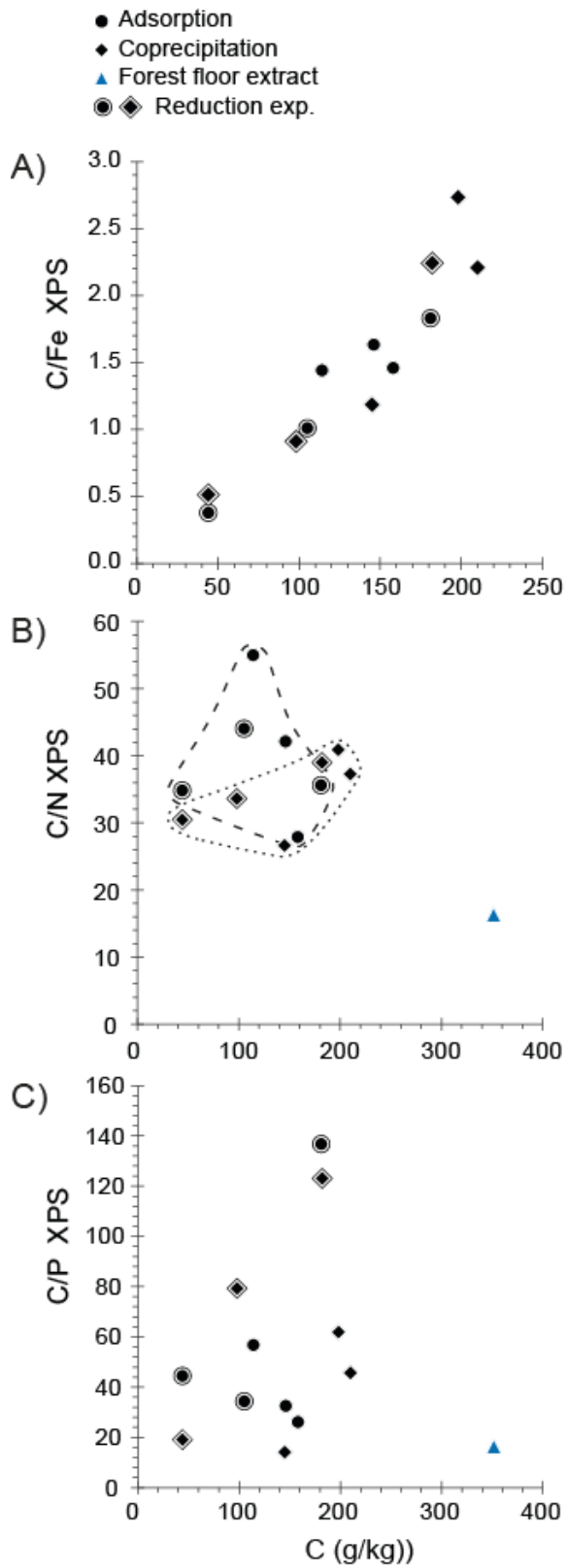
796 Figure 3. Ferrihydrate-associated C (normalized to the specific surface area of 197 m² g⁻¹ of
797 the control ferrihydrate) vs. C in the equilibrium solution. The line represents a BET-isotherm.

798



799

800 Figure 4. Background corrected XPS spectra of the control ferrihydrite Fh (only Fe2p, red),
 801 the forest floor extract FFE (only C1s, N1s, P2p, blue) and the incubated coprecipitates
 802 (CFhD, CFhB, CFhA) and adsorption complexes (AFhD, AFhB, AFhA).



803

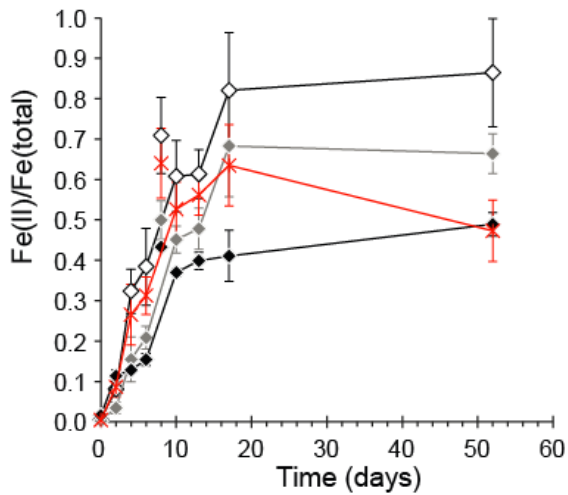
804

805 Figure 5. Comparison of chemical surface composition expressed in XPS intensity ratios
 806 (C/Fe, C/N, and C/P) and bulk C content of Fh-OM associations.

807

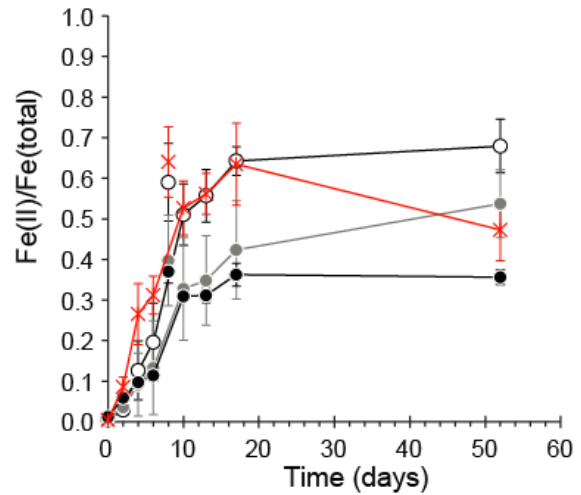
A) Coprecipitation

- C Fh A 44 mg g⁻¹ C
- C Fh B 98 mg g⁻¹ C
- ◆— C Fh D 182 mg g⁻¹ C
- *— Fh control



B) Adsorption

- A Fh A 44 mg g⁻¹ C
- A Fh B 105 mg g⁻¹ C
- ◆— A Fh D 181 mg g⁻¹ C
- *— Fh control



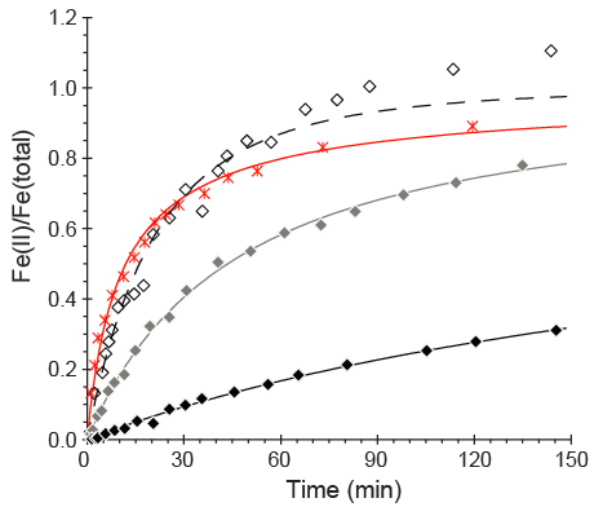
809

810

811 Figure 6. Microbial reduction of ferrihydrite and ferrihydrite-organic matter associations in
 812 *Geobacter bremsensis* cultures. The Fe(II) production was normalized to the total initial
 813 amount of Fe in ferrihydrite. The Fe(II)/Fe(total) of the ferrihydrite control (red stars) at day
 814 52 is much lower than at day 17 and therefore unexpectedly low, letting us assume that this is
 815 due to unintentional oxidation at the end of the experiment in this sample. Error bars represent
 816 standard deviations of triplicate cultures.

A) Coprecipitation

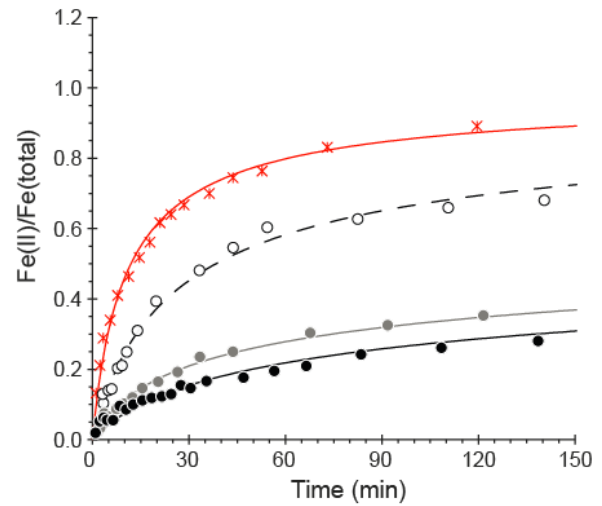
- ◇— C Fh A 44 mg g⁻¹ C
- C Fh B 98 mg g⁻¹ C
- ◆— C Fh D 182 mg g⁻¹ C
- *— Fh control



818

B) Adsorption

- A Fh A 44 mg g⁻¹ C
- A Fh B 105 mg g⁻¹ C
- ◆— A Fh D 181 mg g⁻¹ C
- *— Fh control



819 Figure 7. Abiotic reduction with Na-dithionite: Fe(II) production (normalized to the total
 820 initial Fe in ferrihydrite) versus time. Lines represent the model by Christoffersen and
 821 Christoffersen (1976). Note that the dissolved Fe(II) was estimated to be larger than the total
 822 Fe for sample CFhA, which is unreasonable.